

Suppression of decoherence via strong intra-environmental coupling

Luca Tessieri and Joshua Wilkie

Department of Chemistry, Simon Fraser University, Burnaby, British Columbia V5A 1S6, Canada

(Dated: 9th July 2002)

We examine the effects of intra-environmental coupling on decoherence by constructing a low temperature spin-spin-bath model of an atomic impurity in a Debye crystal. The impurity interacts with phonons of the crystal through Jahn-Teller vibronic coupling. Anharmonic intra-environmental vibrational coupling is incorporated through anti-ferromagnetic spin-spin interactions. The reduced density matrix of the central spin representing the impurity is calculated by dynamically integrating the full Schrödinger equation for the spin-spin-bath model for different thermally weighted eigenstates of the spin-bath. Exact numerical results show that increasing the intra-environmental coupling results in suppression of decoherence. This effect could play an important role in the construction of solid state quantum devices such as quantum computers.

PACS numbers: 03.65.Yz, 03.67.Lx, 05.30.-d

Intra-environmental coupling has customarily been neglected in theoretical models of subsystem-environment interaction. The popular spin-boson model [1, 2], for example, assumes that the environment consists of a set of non-interacting harmonic oscillators linearly coupled to a central spin. The neglect of intra-environmental coupling is motivated more by mathematical convenience than by physical insight.

One failing of such models is that intra-environmental energy transfer can only proceed by using the subsystem as an intermediate. In addition, it is well known that the statistical properties of the energy eigenfunctions and eigenspectra of strongly coupled (irregular) systems is qualitatively different from that of uncoupled (regular) systems. The Wigner functions of eigenvectors for irregular systems are almost uniform over the energetically allowed classical phase space [3]. Those of regular systems are more lumpy with energy localized in a subset of the available modes [4]. Similarly, irregular eigenspectra show level repulsion while regular spectra show level clustering [5]. These spectral signatures have important dynamical consequences [6]. For these reasons coupled environments may have decoherence properties which differ substantially from those predicted by uncoupled oscillator models.

Proposed new technologies such as quantum computing [7], laser control of chemical reactions [8], and molecular electronics [9] all require a qualitative understanding of the effects of decoherence and dissipation for experimental implementation. Predictive theoretical studies for such systems would also greatly benefit from dynamical methods which accurately include the effects of intra-environmental coupling and environmental memory effects.

Unfortunately, exact theories such as the Feynman-Vernon influence functional method [10] and the Nakajima-Zwanzig master equation [11] cannot be easily applied. Approximate theories such as the Redfield [12], completely-positive-dynamical-semigroup [13]

and SRA [14] master equations need testing against exact results before they can be applied with confidence. Thus, exact numerical calculations for subsystems interacting with environments of a small number of degrees of freedom provide the only practical method for exploring the effects of intra-environmental coupling. Such studies would also allow us to test the accuracy of existing master equations.

In this manuscript we report exact numerical results for the decoherence of a central spin interacting with a spin-bath with intra-environmental coupling. The model was constructed to represent an impurity in a thermal crystalline solid; the impurity being the small quantum system and the solid the environment. The first two electronic states of the impurity are vibronically coupled to a number n_s of coupled phonon modes of the crystal. At low temperature the phonon modes can be represented as spin-1/2 modes [15] (representing the first two states of an oscillator) with frequencies sampled from a Debye spectrum with a frequency cutoff (set here at $\omega_D = 1$). With anharmonic phonon-phonon coupling effects included, our model Hamiltonian then takes the form

$$H = \frac{\omega_0}{2}\sigma_z^{(0)} + \beta\sigma_x^{(0)} + \lambda_0\sigma_x^{(0)}\sum_{j=1}^{n_s}\sigma_x^{(j)} + \sum_{j=1}^{n_s}\left[\frac{\omega_j}{2}\sigma_z^{(j)} + \beta\sigma_x^{(j)}\right] + \frac{\lambda}{2}\sum_{i \neq j=1}^{n_s}\sigma_x^{(i)}\sigma_x^{(j)} \quad (1)$$

where we arbitrarily chose $\omega_0 = .8288$ as the frequency of the impurity, $\beta = .01$ is the coefficient of a small anharmonic correction, and $\lambda_0 = 1$ and λ are the subsystem-environment and intra-environmental coupling constants. Terms one, two and four of (1) represent the uncoupled modes of the subsystem (labeled with superscript 0) and environment (labeled with superscripts 1 through n_s). The third term in (1) couples the subsystem and environment, while the last term couples the environment with itself. Here the sigmas represent Pauli matrices. In

our units $\hbar = 1$. [Note that the same Hamiltonian could also represent interacting nuclear or electronic spins in a solid.]

We calculated the reduced density matrix $\rho(t)$ of the impurity via the formula

$$\rho(t) = \begin{pmatrix} \rho_{11}(t) & \rho_{10}(t) \\ \rho_{01}(t) & \rho_{00}(t) \end{pmatrix} = \sum_{m=1}^{n_{\text{eig}}} p_m \text{Tr}_e\{|\psi_m(t)\rangle\langle\psi_m(t)|\} \quad (2)$$

where

$$p_m = \frac{\exp\{-\epsilon_m/kT\}}{\sum_{m=1}^{n_{\text{eig}}} \exp\{-\epsilon_m/kT\}},$$

ϵ_m and $|m\rangle_e$ are the energies and eigenvectors of the isolated environment, and kT is the temperature in units of energy. The notation $\text{Tr}_e\{\hat{\mathbf{A}}\}$ indicates a trace of the operator $\hat{\mathbf{A}}$ over the environmental degrees of freedom. The states $|\psi_m(t)\rangle$ are evolved via the Schrödinger equation from initial states

$$|\psi_m(0)\rangle = |1\rangle_0 \otimes |m\rangle_e \quad (3)$$

under Hamiltonian (1). The basis of eigenstates of the σ_z operators was used to represent all states. The states $|0\rangle$ and $|1\rangle$ represent down and up z-components of the spin, respectively. Thus, the subsystem state $|1\rangle$ in Eq. (3) means that the impurity is initially in its excited state.

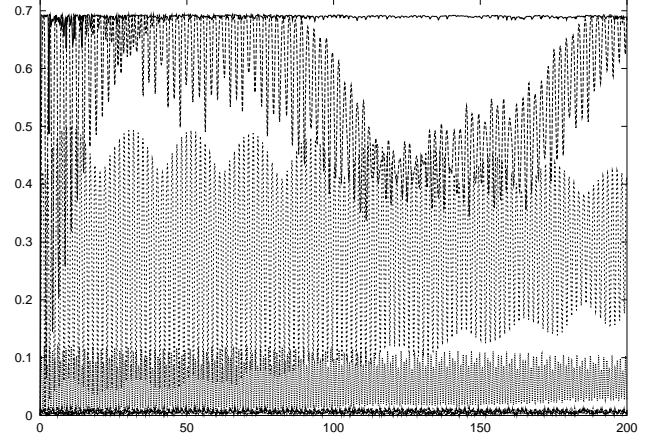
Equations (2) and (3) represent an impurity in a thermal solid which is excited by a fast laser pulse just prior to time $t = 0$ (i.e., a sudden approximation) which then evolves while interacting with phonons in the solid.

The calculations reported here are for $n_s = 12$ bath spins. The ARPACK linear algebra software [16] was used to calculate the lowest $n_{\text{eig}} = 20$ energies and eigenvectors of the isolated environment. A temperature of $kT = .02$ was chosen such that no states with energy quantum number m higher than n_{eig} would be populated at equilibrium. The numerical solution of the Schrödinger ordinary differential equation for $|\psi_m(t)\rangle$ was calculated using an eighth order Runge-Kutta routine [17]. Operations of the Hamiltonian (1) on the wavevector were calculated via repeated application of Pauli matrix multiplication routines. For example

$$\langle j_{n_s}, \dots, j_i, \dots, j_1 | \sigma_x^{(i)} | \psi \rangle = \langle j_{n_s}, \dots, \bar{j}_i, \dots, j_1 | \psi \rangle$$

for all sets of $j_l = 0, 1$, $l = 1, \dots, n_s$ and where $\bar{j}_i = 1$ if $j_i = 0$ and $\bar{j}_i = 0$ if $j_i = 1$. Thus, an operation of $\sigma_x^{(i)}$ simply rearranges the components of $|\psi\rangle$. States of the basis can be represented by integers $j = j_1 + j_2 2 + \dots + j_i 2^{i-1} + \dots + j_{n_s} 2^{n_s-1}$ and since integers are represented in binary form on a computer, the mapping $j \rightarrow j' = j_1 + j_2 2 + \dots + \bar{j}_i 2^{i-1} + \dots + j_{n_s} 2^{n_s-1}$ under $\sigma_x^{(i)}$ can be calculated very simply using Fortran binary-operation intrinsic functions. Operations for $\sigma_y^{(i)}$ and $\sigma_z^{(i)}$ are also straightforward.

Figure 1: Subsystem entropy S versus time t plotted for different values of λ



In Fig. 1 we show the calculated subsystem entropy

$$S(t) = -\text{Tr}_s\{\rho(t) \ln \rho(t)\} = -\frac{1}{2} \ln\{\det[\rho(t)]\} - \frac{1}{2} \sqrt{1 - 4 \det[\rho(t)]} \ln \frac{1 + \sqrt{1 - 4 \det[\rho(t)]}}{1 - \sqrt{1 - 4 \det[\rho(t)]}} \quad (4)$$

where $\det[\rho(t)] = \rho_{11}(t)\rho_{00}(t) - \rho_{10}(t)\rho_{01}(t)$, for various values of the intra-environmental coupling λ . For $\lambda = 0$ (solid curve) the entropy rapidly approaches its maximum value of $\ln(2) \simeq 0.693147\dots$ which corresponds to the diagonalised reduced density matrix

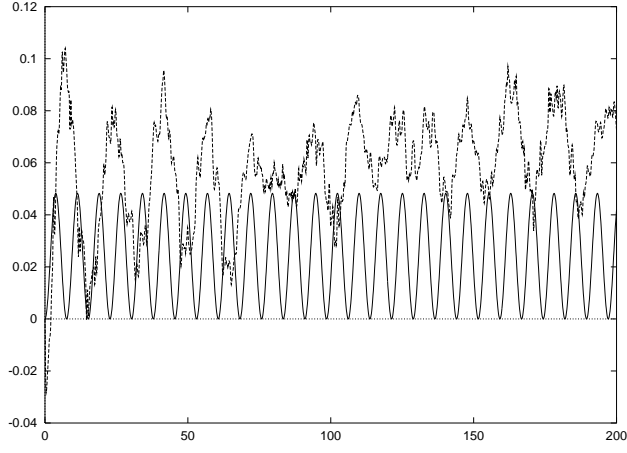
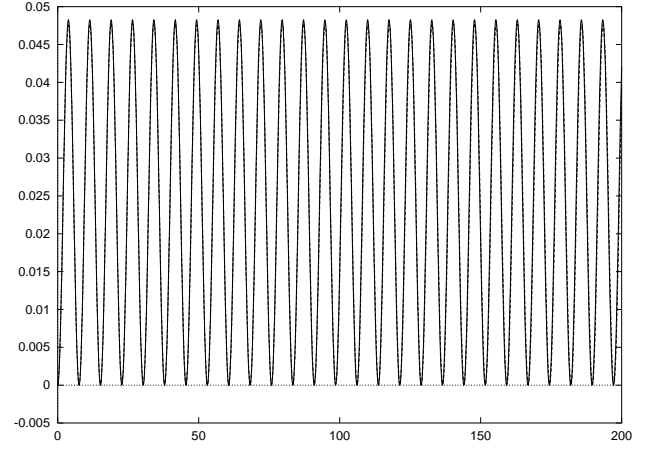
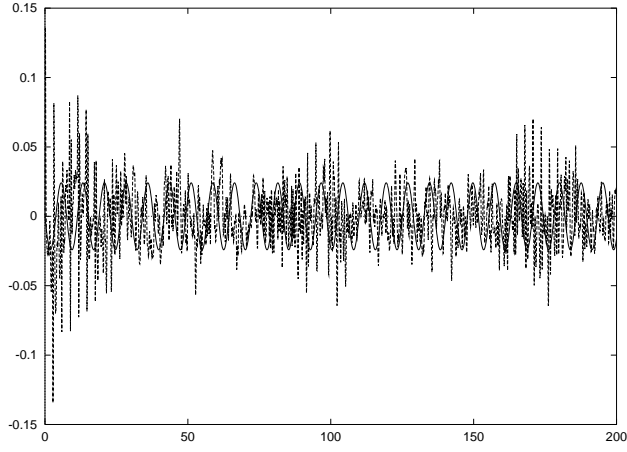
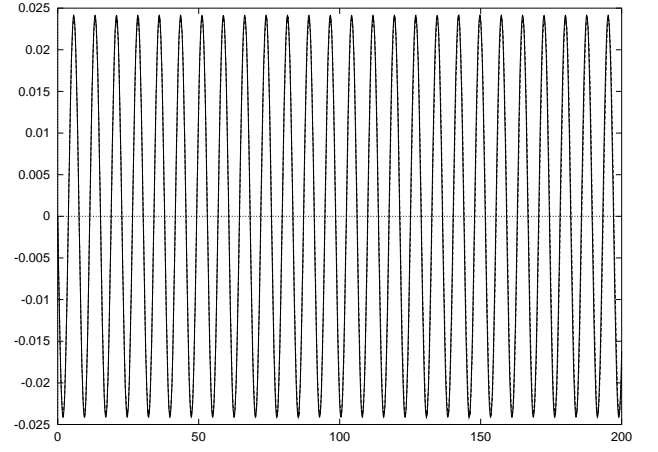
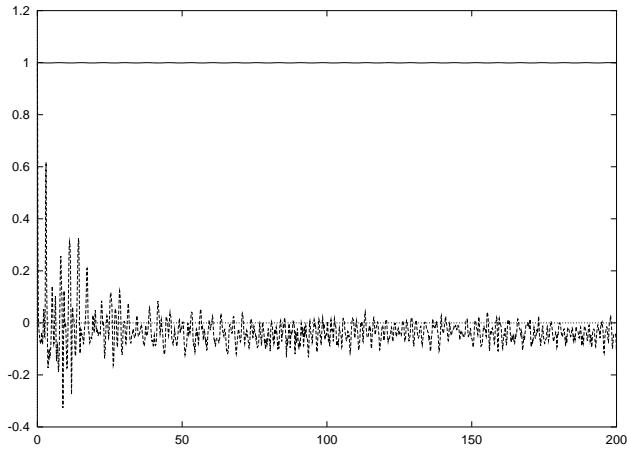
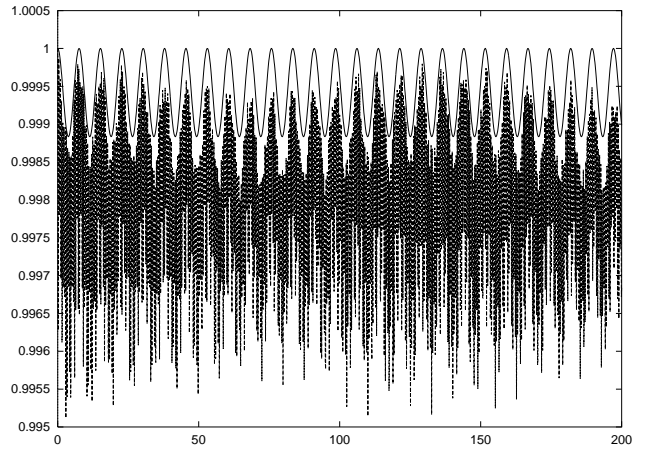
$$\begin{aligned} \rho_{00}(t) &= \rho_{11}(t) = \frac{1}{2} \\ \rho_{10}(t) &= \rho_{01}(t) = 0. \end{aligned}$$

As λ increases through 1 (long dashed curve), 2 (short dashed curve), 4 (dotted curve), and 8 (dot-dashed curve), the entropy approaches a smaller asymptotic value. This strongly suggests that increased intra-environmental coupling suppresses decoherence.

To confirm this we compare the dynamics of the three subsystem spin components

$$\begin{aligned} X(t) &= \text{Tr}_s\{\sigma_x^{(0)} \rho(t)\} = \rho_{10}(t) + \rho_{01}(t) \\ Y(t) &= \text{Tr}_s\{\sigma_y^{(0)} \rho(t)\} = i(\rho_{10}(t) - \rho_{01}(t)) \\ Z(t) &= \text{Tr}_s\{\sigma_z^{(0)} \rho(t)\} = \rho_{11}(t) - \rho_{00}(t) \end{aligned}$$

calculated for Hamiltonian (1) with those of the impurity evolving in isolation (i.e., $\lambda_0 = 0$). In Fig. 2 we show the time evolution of the central spin in the absence of interaction with the bath, i.e., for $\lambda_0 = 0$ (solid line) and the evolution of the same spin for $\lambda_0 = 1$ and $\lambda = 0$ (dashed line), i.e., when the central spin is coupled to a bath of non-interacting spins. As can be seen from Fig. 2(c), the system undergoes rapid decoherence when the interaction with the bath is turned on. In Fig. 3 we show again

(a) $X(t)$ (a) $X(t)$ (b) $Y(t)$ (b) $Y(t)$ (c) $Z(t)$ (c) $Z(t)$ Figure 2: x , y , and z component of the spin versus t for $\lambda = 0$ Figure 3: x , y , and z component of the spin versus t for $\lambda = 8$

the behaviour of $X(t)$, $Y(t)$, and $Z(t)$ for $\lambda_0 = 0$ (solid line, isolated spin) and for $\lambda_0 = 1$ and $\lambda = 8$ (dashed line, central spin coupled to a bath of strongly interacting modes). Here the agreement between the coupled and isolated dynamics is much better than in the previous case; in fact, the only significant discrepancy appears in the behaviour of $Z(t)$, whereas the plots of $X(t)$ and $Y(t)$ for $\lambda_0 = 0$ and $\lambda_0 = 1$ are almost indistinguishable.

Thus, at least in this simple model, increasing anharmonic intra-environmental coupling incrementally suppresses decoherence. There is a relatively simple explanation for the observed behaviour. Define an environmental super-spin with components

$$\Sigma_x = \sum_{j=1}^{n_s} \sigma_x^{(j)}, \quad \Sigma_y = \sum_{j=1}^{n_s} \sigma_y^{(j)}, \quad \Sigma_z = \sum_{j=1}^{n_s} \sigma_z^{(j)},$$

in terms of which Hamiltonian (1) can be rewritten as

$$H = \frac{\omega_0}{2} \sigma_z^{(0)} + \beta \sigma_x^{(0)} + \lambda_0 \sigma_x^{(0)} \Sigma_x + \sum_{j=1}^{n_s} \frac{\nu_j}{2} \sigma_z^{(j)} + \frac{\Omega}{2} \Sigma_z + \beta \Sigma_x + \frac{\lambda}{2} [\Sigma_x^2 - n_s \mathbf{1}], \quad (5)$$

where $\Omega = \sum_{j=1}^{n_s} \omega_j / n_s$ is the average environment frequency and $\nu_j = \omega_j - \Omega$. When $\lambda \gg \Omega$, the last term in (5) dominates the bath Hamiltonian. This entails that the bath eigenstates are nearly eigenvectors of Σ_x ; specifically, the bath eigenstates with lowest energy correspond to the lowest eigenvalues of Σ_x . Since the initial conditions (3) are low-energy bath eigenstates, the evolving dynamical states $|\psi_m(t)\rangle$ remain close to eigenstates of Σ_x with small eigenvalues; as a consequence the central spin becomes nearly decoupled from the environment and its evolution is determined by the effective Hamiltonian

$$H_s \simeq (\omega_0/2) \sigma_z^{(0)} + (\beta + \lambda_0 s_x) \sigma_x^{(0)}$$

where s_x is a (typically small) eigenvalue of Σ_x .

Our study strongly suggests that intra-environmental coupling has as important an effect on decoherence as temperature or subsystem-environmental coupling. Environments of N (coupled oscillator) phonons should have similar decoherence properties. Since the Wigner functions of the energy eigenstates of strongly coupled systems are nearly uniform over the classical energy surface [3], energy is distributed equally among all modes. Thus displacements from equilibrium of any phonon mode must be small at low temperature, especially in the thermodynamic limit. Since the coupling of an impurity to a phonon is through its displacement coordinate, this coupling will also be small. By contrast, energy distribution in uncoupled oscillator systems is non-uniform and may be localized in a small number of modes [4]. Hence vibronic coupling to these modes will be strong as will decoherence.

We have obtained similar results for both larger and smaller numbers of bath spins and also in the case of ferromagnetic intra-environmental coupling. We believe that our model is a reasonably accurate representation of an impurity in a low-temperature crystal. If such strong intra-environmental coupling exists in nature, it could be exploited as a platform for quantum computing. We are currently developing methods for the study of higher-temperature systems where environmental modes are modeled by coupled harmonic oscillators.

The authors gratefully acknowledge the financial support of the Natural Sciences and Engineering Research Council of Canada.

-
- [1] A. J. Leggett, S. Chakravarty, A. T. Dorsey, M. P. A. Fisher, A. Garg and W. Zwerger, *Rev. Mod. Phys.*, **59**, 1 (1987).
 - [2] U. Weiss, *Quantum dissipative systems, 2nd Ed.*, (World Scientific, Singapore, 1999).
 - [3] M.V. Berry, *Proc. R. Soc. Lond. A*, **423**, 219 (1989).
 - [4] O. Bohigas, S. Tomsovic and D. Ullmo, *Phys. Rep.*, **223**, 43 (1993).
 - [5] M.V. Berry in *Chaotic behavior in quantum systems*, eds. G. Iooss, R. H. G. Helleman and R. Stora, (North-Holland, Amsterdam, 1983).
 - [6] J. Wilkie and P. Brumer, *J. Chem. Phys.*, **107**, 4893 (1997); *Phys. Rev. Lett.*, **67**, 1185 (1991).
 - [7] H.-K. Lo, S. Popescu and T. Spiller, *Introduction to quantum computation and information*, (World Scientific, Singapore, 1998).
 - [8] P. Brumer and M. Shapiro, *Laser and Particle Beams*, **16**, 599 (1998).
 - [9] V. Mujica, A. Nitzan, Y. Mao, W. Davis, M. Kemp, A. Roitberg and M.A. Ratner, *Adv. Chem. Phys.*, **107**, 403 (1999).
 - [10] R. P. Feynman and F. L. Vernon, Jr., *Annals of Physics*, **24**, 118 (1963).
 - [11] S. Nakajima, *Prog. Theor. Phys.*, **20**, 948 (1958); R. Zwanzig, *J. Chem. Phys.* **33**, 1338 (1960); R. Zwanzig, in *Lectures in Theoretical Physics*, Vol. 3 (Interscience, New York, 1961).
 - [12] A. Suárez, R. Silbey and I. Oppenheim, *J. Chem. Phys.*, **97**, 5101 (1992); V. Romero-Rochin and I. Oppenheim, *J. Stat. Phys.*, **53**, 307 (1988); *Physica A*, **155**, 52 (1989); V. Romero-Rochin, A. Orsky and I. Oppenheim, *ibid.* **156**, 244 (1989); A.G. Redfield, *Adv. Magn. Reson.*, **1**, 1 (1965).
 - [13] G. Lindblad, *Commun. Math. Phys.*, **48**, 119 (1976); V. Gorini, A. Kossakowski, and E. C. G. Sudarshan, *J. Math. Phys.*, **17**, 821 (1976); R. Alicki and K. Lendi, *Quantum Dynamical Semigroups and Applications*, (Springer, Berlin, 1987).
 - [14] J. Wilkie, *J. Chem. Phys.*, **115**, 10335 (2001); *J. Chem. Phys.*, **114**, 7736 (2001); *Phys. Rev. E* **62**, 8808 (2000).
 - [15] N.V. Prokof'ev and P.C.E. Stamp, *Rep. Prog. Phys.*, **63**, 669 (2000).
 - [16] See <http://www.caam.rice.edu/software/ARPACK/>.
 - [17] DOP853.f, E. Hairer and G. Wanner, <http://elib.zib.de/pub/elib/hairer-wanner/nonstiff/>.